

Racial differences in genomic features and new trans-ancestry prognosis subtypes in bladder cancer

Baifeng Zhang (✉ zhangbaifeng1@gmail.com)

The University of Hong Kong <https://orcid.org/0000-0003-1966-2285>

Peilin Jia

Jiayin Wang

Xi'an Jiaotong University

Guangsheng Pei

The University of Texas Health Science Center at Houston, Houston <https://orcid.org/0000-0003-1804-7598>

Changxi Wang

Shimei Pei

Xiangchun Li

Tianjin Medical University Cancer Institute and Hospital

Shuai Ding

Zhongming Zhao

The University of Texas Health Science Center at Houston <https://orcid.org/0000-0002-3477-0914>

Xin Yi

Yi Huang

Article

Keywords:

Posted Date: December 27th, 2021

DOI: <https://doi.org/10.21203/rs.3.rs-1157888/v1>

License:   This work is licensed under a Creative Commons Attribution 4.0 International License.

[Read Full License](#)

1 **Racial differences in genomic features and new trans-ancestry prognosis subtypes in**
2 **bladder cancer**

3

4 Baifeng Zhang^{1,2,3*}, Peilin Jia⁴, Jiayin Wang⁵, Guangsheng Pei⁴, Changxi Wang³, Shimei
5 Pei³, Xiangchun Li⁶, Shuai Ding⁷, Zhongming Zhao⁴, Xin Yi³, Yi Huang^{3,5,8*}

6

7 ¹Departments of Clinical Oncology, The University of Hong Kong-Shenzhen Hospital,
8 Shenzhen, 518053, China

9 ²Departments of Clinical Oncology, Li Ka Shing Faculty of Medicine, The University of
10 Hong Kong, Hong Kong, China

11 ³Geneplus-Beijing, Beijing 102206, China

12 ⁴Center for Precision Health, School of Biomedical Informatics, The University of Texas
13 Health Science Center at Houston, Houston, TX 77030, USA

14 ⁵Department of Computer Science and Technology, School of Electronic and Information
15 Engineering, Xi'an Jiaotong University, Shaanxi 710049, China

16 ⁶Department of Epidemiology and Biostatistics, Tianjin Medical University Cancer Institute
17 and Hospital, Tianjin 300060, China

18 ⁷ School of Management, Ministry of Education Key Laboratory of Process Optimization and
19 Intelligent Decision-Making, Hefei University of Technology, Hefei, 230009, China

20 ⁸Luohu people's hospital, Shenzhen, 518000, China

21

22 *Correspondence: zhangbaifeng1@gmail.com; huangyi@geneplus.org.cn

23

24

25

26 **ABSTRACT**

27

28 The incidence and survival of bladder cancer vary greatly among different populations but
29 the influence of the associated molecular features and evolutionary processes on its clinical
30 treatment and prognostication remains unknown. Here, we analyze the genomic architectures
31 of over 500 bladder cancer patients from Asian/Black/White populations. We identify novel
32 association between *AHNAK* mutations and APOBEC-a mutational signature whose activities
33 vary substantially across populations. All significantly mutated genes but only half of arm-
34 level somatic copy number alterations (SCNAs) are enriched with clonal events, indicating
35 large-scale SCNAs as rich sources fostering bladder cancer clonal diversities. The prevalence
36 of *TP53* and *ATM* clonal mutations as well as the associated burden of SCNAs is
37 significantly higher in Whites/Blacks than in Asians. We identify a trans-ancestry prognostic
38 subtype of bladder cancer characterized by: enrichment of non-muscle-invasive patients and
39 muscle-invasive patients with good prognosis, increased *CREBBP/FGFR3/HRAS/NFE2L2*
40 mutations, decreased intra-tumor heterogeneity and genome instability and activated tumor
41 microenvironment.

42

43 **INTRODUCTION**

44

45 Bladder cancer is the sixth most common type of adult cancer with almost 430, 000 new
46 cases diagnosed per year¹. Bladder cancer is classified into non-muscle invasive bladder
47 cancer (NMIBC) and muscle-invasive bladder cancer (MIBC) according to their
48 histopathological features and clinical behaviors. NMIBC, the major subtype of bladder
49 cancer that accounts for 70% to 80% of all newly diagnosed cases, has better overall survival
50 but high recurrence rate of 31-78% while the rest of patients with muscle-invasive or

51 metastatic diseases exhibit quite low survival rate^{2,3}. The genetic or molecular basis
52 underlying such great disparities in clinical outcomes between NMIBC and MIBC remains
53 largely unclear.

54

55 NMIBC and MIBC are supposed to develop through different evolutionary paths on distinct
56 genetic background. The genetic architecture of MIBC has become increasingly clear with
57 the accomplishment of several large-scale genome sequencing projects in large cohorts of
58 MIBC patients⁴⁻⁶. Characterization of the genetic causes of NMIBC by large-scale
59 approaches had only been performed in a relatively small number of patients^{7,8}. These studies
60 identified a number of new driver events, such as truncating mutations of the chromatin
61 remodeling genes (*UTX*, *MLL-MLL3*, *ARID1A* and others) and recurrent fusions involving
62 *FGFR3* and *TACC3*, in addition to the well-known TP53-RB1 and FGFR3-Ras pathways that
63 are mutated frequently in MIBC and NMIBC, respectively^{7,8}. Bladder cancer is a
64 heterogeneous group of diseases with distinct subtypes exhibiting different mutational
65 signatures and expression features⁴. However, these studies primarily focused on the somatic
66 events with elevated mutation frequencies among different patients or subtypes⁵⁻⁸.

67

68 The degrees of intra- and inter-tumor heterogeneities can be assessed by analyzing the
69 genomic architectures of individual bladder cancer patients. One previous study analyzing the
70 clonality of MIBC in a small number of pre and post-chemotherapy samples revealed that the
71 extensive and dynamic clonal evolution found in MIBC patients may lead to chemotherapy
72 resistance⁹. It was expected that the genomic architectures would have great influence on the
73 clinical outcomes of bladder cancer and somatic driver events acquired at different
74 evolutionary stages would also have different prognostic values. However, few of the genetic
75 prognostic biomarkers for bladder cancer had been developed utilizing their clonal or sub-

76 clonal states in large cohorts of patients with different genetic background, despite of the
77 well-documented disparities in bladder cancer risk and survival across races/ethnics in
78 epidemiological studies¹⁰. Whites are more than twice likely to develop bladder cancer than
79 Blacks while Asian Americans have lower risk of developing bladder cancer than Whites and
80 Blacks¹¹. The clinical outcomes of bladder cancer also exhibit racial disparities with shorter
81 survival observed in Blacks¹⁰. Moreover, these previous prognostic studies also focused only
82 on single level of molecular data and no study had characterized the overall genomic
83 architectures of individual bladder cancer patients based on both large-scale somatic copy
84 number alterations (SCNAs) and single nucleotide variants (SNVs) simultaneously to stratify
85 distinct prognostic subtypes. In the study, we tried to investigate that with disparities in
86 genetic background, life history and mutagens exposure, whether bladder cancer patients
87 from different populations might show different mutational signatures and therefore further
88 lead to discrepancies in mutational features and genomic architectures.

89
90 To more comprehensively understand the genetic diversities of bladder cancer, we collect
91 large-scale genomic data from The Cancer Genome Atlas (Cohort 1: TCGA-BLCA)^{4,6} and
92 the Chinese population (Cohort 2: Chinese-BLCA)^{7,8}. Cohort 1 consists of MIBC patients
93 from three different racial populations (White, Black and Asian) and Cohort 2 consists of
94 both MIBC and NMIBC patients from Asia only. We use the MIBC or NMBIC patients from
95 Cohort 2 separately or jointly to test or validate some of the findings observed in Cohort 1. In
96 total, our study cohorts include 468 MIBC and 37 NMIBC patients. We compare the
97 differences in mutational signatures among Asian, Black and White populations and further
98 characterize the association between driver gene mutations and the activities of mutational
99 signatures. We perform prognostic analysis of MIBC in Cohort 1 patients with survival
100 information available and further cluster the MIBC and NMBIC patients according to their

101 molecular patterns. After quantifying the cancer cell fractions (CCFs) of all potential
102 prognostic somatic events, we categorize the bladder cancer patients into distinct prognostic
103 subtypes showing differences in intratumor heterogeneity, genome instability, metastatic
104 ability and immune features.

105

106 **RESULTS**

107

108 **Racial differences in mutational signatures**

109 To dissect the somatic mutation landscapes of the 505 bladder cancer patients in our study,
110 Mutect2¹² and ReCapSeg¹³ were used to call somatic mutations and allelic SCNAs with the
111 whole-exome sequencing data. After further filtering steps (Online Methods), 136, 346
112 somatic mutations (132, 100 SNVs and 4, 246 short insertions/deletions (Indels)) and 21, 779
113 SCNA segments were generated for downstream analysis. We then inferred the CCFs of
114 SNVs and SCNAs simultaneously for each patient. By combining all somatic events from all
115 patients, 11.2% of SNVs, 30.5% of Indels and 41.1% of SCNAs were identified as sub-clonal
116 events (Supplementary Table 1).

117

118 The mutational signatures document the evolutionary history of interactions between multiple
119 exogenous and endogenous mutational processes which consequently result in the
120 accumulation of somatic mutations in tumor cells. Bladder cancer patients from different
121 populations may have distinct genetic background, life history or mutagen exposure. To
122 investigate whether there were any racial differences in mutational signatures during bladder
123 cancer evolution, we first divided our study cohorts into three populations of Asian (140),
124 Black (23) and White (324) origins. We extracted the mutational signatures from SNVs with
125 Bayesian non-negative matrix factorization (NMF). We identified five signatures in Asian,

126 two signatures in Black and four signatures in White (**Fig. 1a** and **Supplementary Fig. 1**).
127 Through clustering analysis of the cosine similarities and Pearson correlation values between
128 these signatures and the 30 Sanger signatures with reported roles in mutagenesis^{14–16}, the five
129 mutational signatures identified in our cohorts could be grouped into categories resembling
130 the APOBEC-a, APOBEC-b, ERCC2 & AGE, ARISTOLOCHIC and MMR Sanger
131 signatures (cosine similarities between 0.68 and 0.97, **Fig. 1a**, **Supplementary Fig. 2** and
132 **Supplementary Data 1**). APOBEC-a and APOBEC-b signatures, accounting for the
133 majority of mutations in bladder cancer, appeared to be more likely to occur early during
134 bladder cancer development⁴. The ERCC2 & AGE signature included one signature mediated
135 by *ERCC2* mutations¹⁷ and another signature correlated with the age of cancer diagnosis.
136 ARISTOLOCHIC signature was related to exposures to aristolochic acid. The last mutational
137 signature showed relatively low similarity (cosine similarity of 0.68) to the MMR signature
138 which had not been reported in bladder cancer previously.

139

140 Of these five signatures, the activities of both APOBEC-a and ERCC2 & AGE signatures
141 were the highest in White and the lowest in Asian, regardless of the clonal/sub-clonal states
142 of mutations ($P < 0.001$ & $FDR < 0.1$, **Fig. 1b**). The ARISTOLOCHIC and MMR-like
143 signatures occurred only in Asian and were both enriched in the sub-clonal state ($P < 0.001$ &
144 $FDR < 0.1$, **Fig. 1b** and **Supplementary Fig. 3**). These observations might suggest the
145 presence of population variations in mutational processes operating at different evolution
146 stages during bladder cancer development. To further assess the potential clinical association
147 of these mutational signatures, we performed unsupervised clustering of the patients in
148 Cohorts 1 and 2 according to their mutational signature activities and identified four
149 mutational signature clusters (MSig1 to MSig4, **Fig. 1c**). Different clusters of patients
150 showed varied activities of different mutational signatures (**Fig. 1d**) and were associated with

151 distinct clinical outcomes (**Fig. 1e**, $P = 0.002$). Cluster MSig2 showed enrichment in Asian
152 patients (**Fig. 1c**) and had high MMR-like signature activity ($P < 0.001$ & $FDR < 0.1$, **Fig.**
153 **1d**). Prognostic analysis of Cohort 1 revealed that MIBC samples in cluster MSig2 tended to
154 have the shortest overall survival (**Fig. 1e**) and this observation had to be further investigated
155 in future studies as the number of samples with survival information available in cluster
156 MSig2 was quite small in our study. Patients in the MSig3 and MSig4 clusters had high
157 levels of APOBEC and *ERCC2* & AGE signature mutagenesis (**Fig. 1d**), respectively.
158 Multivariate Cox regression analysis of Cohort 1 patients showed that those patients in the
159 MSig3 and MSig4 clusters had better survival than those belonging to MSig1 cluster (**Fig.**
160 **1f**).

161

162 The Asian cohort in our study was consisted of patients from both Europe/USA areas (Cohort
163 1: MIBC) and Asia areas (Cohort 2: MIBC and NMIBC) and we compared the relative
164 contribution of the mutational signatures among these three Asian patient groups and found
165 that the activities of APOBEC-a and -b signatures were relatively higher in MIBC patients
166 from Cohort 2 than the other two groups of Asian patients. Both MIBC and NMIBC patients
167 from Cohort 2 showed significantly high levels of MMR-like signature activities compared
168 with MIBC samples from Cohort1 (**Supplementary Fig. 3**). Nevertheless, more studies and
169 samples were needed to validate the observed racial differences in the activity of MMR-like
170 signature and we could not rule out the potential influence of study batch effect on this
171 observation due to the following reasons: (i) the MMR-like signature with minor exposures
172 could only be observed in Cohort 2 generally; (ii) most of the mutations contributed to the
173 MMR-like signature were subclonal; (iii) the MMR-like signature had a relatively low level
174 of similarity to any known COSMIC signatures; and (iv) little previous evidence suggested
175 the presence of this signature in bladder cancer (**Supplementary Fig. 4**).

176

177 **Gene mutations potentially associated with signature activities**

178 To explore whether there were any genes whose mutations were associated with the
179 mutational signature activities, we performed signature enrichment analysis for those genes
180 mutated at elevated frequencies with permutation tests which could control the inflation that
181 an increase in the overall mutation burden in each sample or in the total number of mutations
182 in each gene usually correlated with increased signature activity. To determine the
183 significance level of associations between the elevated mutation frequency of each gene and
184 the increased activity of each signature, the mutation burden attributed to a given signature
185 from tumors that harbored non-silent mutations in the gene was compared with tumors that
186 did not by combining the two study cohorts (Online Methods).

187

188 Consistent with previous reports¹⁷, we showed that *ERCC2* mutation state and smoking were
189 significantly correlated with *ERCC2* & AGE signature activity (FDR < 0.1, $P < 0.001$, **Fig**
190 **2a, b**). Interestingly, we also found that *ERCC2* mutation state was correlated with the
191 activity of APOBEC-b signature (FDR < 0.1), with an increase of 75 APOBEC-b mutations
192 in *ERCC2*-mutant patients (**Fig. 2b**). Notably, we identified that the APOBEC-a signature
193 activity, an indicator of good clinical outcome in bladder cancer⁴, was associated with
194 *AHNAK* mutations which appeared to act as a tumor suppressor through potentiating the
195 TGF β signalling in a previous study at the protein level¹⁸ (**Fig. 2a**). The median numbers of
196 APOBEC-a mutations in patients with and without non-silent *AHNAK* mutations were 235
197 and 62, respectively (**Fig. 2b**, $P < 0.001$). Correlation between *HRAS* mutation states and the
198 MMR-like signature activity was also noticed in our study (**Fig. 2a, b**).

199

200 We further validated that whether racial differences in mutation frequencies of several key
201 genes or pathways may partially account for the racial differences in mutational signature
202 activities among Asian/Black/White populations by combining Cohorts 1 and 2. The
203 frequency of *AHNAK* mutations was the highest in the White patients who also showed the
204 highest APOBEC-a signature activity (9.6% in White vs 4.3% in Black & 6.4% in Asian)
205 while the frequency of *HRAS* mutations was the highest in the Asian patients (14.3% in Asian
206 vs 0.0% in Black & 3.4% in White) (**Fig. 2c**). At the pathway level, genes involved in the
207 DNA polymerase pathway and other conserved DNA damage response genes also had the
208 highest mutation frequencies in White population (**Supplementary Fig. 5a**).

209

210 To determine whether low-frequency mutations in genes involved in the DNA damage
211 responses were linked to mutational signature activities, we performed permutation tests for
212 the DNA damage response pathways from curated databases (Online Methods). We observed
213 that mutations of the nucleotide excision repair (NER) pathway which includes the *ERCC2*
214 gene were significantly associated with the activities of both ERCC2 & AGE and APOBEC-b
215 signatures (**Supplementary Fig. 5b**). Mutations in the DNA polymerase pathway were
216 identified to be associated with the APOBEC-a signature activity. Additionally, mutations of
217 a group of genes defined as other conserved DNA damage response genes were significantly
218 associated with the mutagenesis of three signatures, APOBEC-a, APOBEC-b and ERCC2 &
219 AGE (**Supplementary Fig. 5b, c**).

220

221 We next compared the expression levels of *AHNAK*, *ERCC2* and *HRAS* among the three
222 racial populations in Cohort 1. We observed that the expression levels of both *AHNAK* and
223 *ERCC2* were significantly lower in Asian than those in White population ($P < 0.05$ and $P <$
224 0.001 , respectively) (**Supplementary Fig. 6**), which provided further evidence supporting

225 that racial differences in the activities of *AHNAK* and *ERCC2* might contribute to the
226 observed racial differences in the prevalence of APOBEC-a and ERCC2 & AGE signatures
227 in bladder cancer. However, *HRAS* expression showed no significant difference among
228 different race groups (**Supplementary Fig. 6**).

229

230 **Racial disparities in cancer gene mutations and SCNAs**

231 To depict the racial disparities in molecular features among different racial groups, we first
232 identified the significantly mutated genes (SMGs) by combining all samples from the two
233 study cohorts and then compared the prevalence of mutations in SMGs among different race
234 groups. A total of 57 SMGs were identified by MutSig2CV ($q < 0.1$) (**Supplementary Data**
235 **2**) and 26 of them were cancer census genes that were expressed in over 75% of TCGA
236 patients (supported by at least three read counts) and were kept for downstream analysis¹⁹.
237 Five of the 26 SMGs had not been reported as SMGs in bladder cancer in previous
238 studies^{6,20–22}: *CDKN1B* (1.2%), *ITK* (1.8%), *PRDM2* (3.1%), *FOXA1* (2.7%) and *BAP1*
239 (1.8%). A total of 34 frequent arm-level SCNAs occurred in at least 30% of patients by
240 combining the two study cohorts.

241

242 The prevalence of clonal mutations in several SMGs varied substantially among different race
243 groups. Both Black and White patients showed higher fractions of clonal *TP53* mutations
244 than Asian patients from Cohorts 1 and 2. The frequencies of clonal mutations in *HRAS* in
245 Asian patients from Cohorts 1 and 2 were consistently higher than Whites. Compared with
246 Asian patients, clonal mutations in *ATM* and *ARID1A* showed higher prevalence in Blacks
247 and Whites, respectively. The frequency of *NRAS* mutations was higher in Blacks than
248 Whites and three genes, including *FGFR3*, *ELF3* and *TSC1*, showed higher frequencies of
249 clonal mutations in Whites than in Asian patients from Cohort 2. Interestingly, *FGFR3* clonal

250 mutations were observed to occur more frequently not only in Asian patients in Cohort 1 than
251 in Cohort 2. *FGFR3* mutations are the early driver events during NMIBC evolution and we
252 also observed that *FGFR3* clonal mutations occurred more frequently in NMIBC than in
253 MIBC in Cohort 2 patients²³ (**Fig. 3a, b**).

254

255 We next compared the overall burden of SCNAs at the chromosome/arm/focal levels across
256 different racial groups (Online Methods). NMIBC patients generally had a lower burden of
257 SCNAs at the chromosome/arm levels than the MIBC patients. The overall arm- or
258 chromosome-level SCNA scores in Asian MIBC patients were lower than those in White or
259 Black MIBC patients (**Fig. 3c**). This observation was consistent with the finding of low
260 prevalence of clonal mutations in the *TP53* and *ATM* gatekeeper genes governing DNA repair
261 in Asian MIBC patients. We further categorized each chromosome/arm level SCNA into
262 clonal or subclonal event and found that the majority of arm-level deletions either in clonal or
263 subclonal states showed substantial inter-population variations in their prevalence. A large
264 number of chromosomes/arms showed higher prevalence of clonal deletions in White/Black
265 MIBC patients than in the Asian MIBC patients. We also observed a large number of
266 chromosomes/arms showing higher prevalence of subclonal SCNAs in Whites than in Asian
267 patients from Cohort 2 (**Fig. 3d**). Moreover, we observed that only quite a few number of
268 clonal arm-level SCNAs, including del(3p) and amp(20), had higher prevalence but a number
269 of subclonal SCNAs showed significantly lower prevalence in Asian MIBC patients from
270 Cohort 2 than in Asian patients from Cohort 1 (**Fig. 3e**).

271

272 It has been reported that bladder cancer patients with different genetic backgrounds may be
273 presented with different disease stages at the time of diagnosis¹⁰. In our study cohorts, we
274 also observed that MIBC patients of Asian origins had higher prevalence of low-stage disease

275 while Blacks and Whites had higher prevalence of high-stage disease (**Supplementary Fig.**
276 **7**). To correct for the potential influence of heterogeneities in disease stages on the racial
277 disparities in genomic features of MIBC, we further analyzed the racial differences in the
278 mutation landscapes and SCNA profiles in low-staged (staged I & II) MIBC patients due to
279 the lack of sufficient numbers of high-staged patients in the Asian cohorts. Again, the
280 prevalence of clonal mutations in *TP53* and *ATM* was significantly higher in Whites and
281 Blacks than in Asians, respectively, among MIBC patients with low-stage disease
282 (**Supplementary Fig. 8**). The prevalence of clonal mutations in *NFE2L2* was the highest in
283 low-staged Black patients and the fractions of White patients harboring clonal mutations in
284 *FGFR3*, *TSC1* and *CDKN2A* were significantly higher than those of Asian patients from
285 Cohort 2. Clonal mutations in *HRAS* also showed significantly higher prevalence in Asians
286 than in Whites among the low-staged patients. We also confirmed that the prevalence of
287 *FGFR3* clonal mutations was significantly higher in Asians from Cohort 1 than in Asians
288 from Cohort 2 among the low-stage MIBC patients. The trends of higher prevalence of clonal
289 deletions and subclonal SCNAs in Whites or Blacks were also observed among patients with
290 low stage MIBC. Differences in the frequencies of clonal deletions of several chromosome
291 arms including del(3p) and subclonal SCNAs affecting a number of other arms were also
292 observed between Asians from Cohorts 1 and 2 among the low-staged patients.

293

294 **Genomic architectures and subtypes of bladder cancer**

295 Our study included a large number of bladder cancer patients with different genetic
296 backgrounds and we then tried to perform molecular subtyping of bladder cancer by
297 integrating multiple somatic events according to their CCFs in all samples by combining
298 Cohorts 1 and 2. We inferred the genomic architectures of bladder cancer by focusing on the
299 26 SMGs with reported roles in the Cancer Gene Census database and the 34 frequent arm-

300 level SCNAs altered in at least 30% of patients as defined above. To explore the contribution
301 of these SMGs and frequent arm-level SCNAs during bladder cancer evolution, we estimated
302 the CCF of each SMG and SCNA in each sample. Overall, the median CCFs of SMGs were
303 higher than those of SCNAs by combining the two study cohorts (**Fig. 4a**). All the 26 SMGs
304 were found to be enriched with clonal non-silent mutations (FDR < 0.1) while only about
305 50% (17/34) and 15% (5/34) of the frequent arm-level SCNAs were significantly enriched
306 with clonal and sub-clonal events (FDR < 0.1), respectively (**Fig. 4a**). These data suggested
307 that heterogeneities in the genomic architectures of bladder cancer were more likely to arise
308 from diversity in the clonality of arm-level SCNAs.

309

310 Few previous studies evaluated the prognostic values of individual somatic events according
311 to their clonal or subclonal states in bladder cancer. Nevertheless, somatic alterations
312 affecting each individual SMG and SCNA usually could only be detected in a minor fraction
313 of samples and stratification of them into clonal or subclonal events would further reduce the
314 numbers of patients harboring alterations in prognosis analysis. We did not observe
315 significant differences in the clinical outcomes of different racial groups in Cohort 1, which
316 may be partially due to the lack of sufficient number of Asian and Black patients with their
317 survival information available (**Supplementary Fig. 9**). Thus, we further evaluated the
318 prognostic value of the SMGs and frequent SCNA events according to their clonal or sub-
319 clonal states by ignoring the racial origins of the patients to increase the sample sizes. We
320 combined the different racial groups in Cohort 1 together in Kaplan-Meier analysis and
321 multivariate Cox regression analysis. In total, we identified only four individual events with
322 potential prognostic value in Cohort 1 (**Table 1, Supplementary Data 3**). Cohort 1 patients
323 with *KRAS* mutations, all of which were clonal, had poor clinical outcome while clonal

324 deletions of either 21q or 12p and sub-clonal deletions of 18p were associated with shortened
325 overall survival in Cohort 1.

326

327 We next tried to stratify whether there were any subtypes of bladder cancer whose overall
328 genetic architectures had great influence on their clinical outcomes. We performed NMF
329 analysis of the CCFs of the 26 SMGs and 34 arm-level SCNAs by combining the two study
330 cohorts. In total, we identified two molecular subgroups (termed as clusters A and B), whose
331 clinical outcomes were divergent. Because long-term survival information was not available
332 for the patients from Cohort 2, we performed survival analysis for all the MIBC samples in
333 the TCGA dataset. TCGA MIBC patients in cluster A had worse survival rate than those in
334 cluster B (**Fig. 4b**) (HR = 1.64, 95% CI: 1.14 ~ 2.36; $P = 0.007$). Multivariate analysis further
335 proved that the genomic architectures could predict the clinical outcomes of bladder cancer
336 patients independently by adjusting for age, gender, TNM stage and mutational signature
337 (**Fig. 4c**). Further comparison of these two genomic subtypes with the molecular subtypes
338 defined by TCGA at different expression levels showed that genomic cluster B tended to be
339 clustered with the molecular subtypes mRNA_Luminal_papillary, lncRNA_3, miRNA_3 and
340 RPPA_1 in Cohort 1 patients²⁰ (**Supplementary Fig. 10**). It had been shown previously that
341 bladder cancer patients exhibiting the Luminal_papillary signature at the mRNA level had
342 low risk of disease progression²⁰. Patients belonging to either the miRNA subtype 3 which
343 was correlated with the lncRNA_3 signature or the RPPA cluster 1 showed the best survival
344 in previous TCGA analysis²⁰. Overall, our analysis at the genomic level provided further
345 evidence complementary to the previously defined molecular subtypes of bladder cancer at
346 the expression levels.

347

348 **Molecular features of prognostic subtypes defined by genomic architectures**

349 To understand which factors contributed to the distinct prognosis of bladder cancer subtypes
350 defined by genomic architectures, we compared the prevalence of 60 potential driver events
351 (26 SMGs and 34 arm-level SCNAs) between clusters A and B. We showed that four SMGs
352 (*CREBBP*, *FGFR3*, *HRAS* and *NFE2L2*) but none of the frequent arm level SCNAs had
353 significantly higher prevalence of genetic aberrations in cluster B patients who had better
354 prognosis than in cluster A patients (FDR < 0.1, **Fig. 4a** and **Supplementary Data 4**). On the
355 other hand, three SMGs (*TP53*, *RBI* and *PRDM2*) and about 91% of the frequent arm level
356 SCNAs were enriched with alterations in cluster A patients who showed poor prognosis
357 (FDR < 0.1, **Fig. 4a** and **Supplementary Data 4**). Notably, of the SMGs mutated more
358 frequently in cluster B than in cluster A, three showed race-specific enrichment of clonal
359 mutations among the low-staged patients with *FGFR3*, *HRAS* and *NFE2L2* mutations being
360 enriched in Whites/Asians from Cohort 2, Asians from the two study cohorts and Blacks,
361 respectively (**Fig. 4a**). These observations indicated that trans-ancestry analysis of the
362 genomic architecture of bladder cancer may be effective in screening out the trans-ancestry
363 prognostic subtypes.

364

365 We inferred the potential temporal ordering of the acquisitions of SMGs and frequent arm-
366 level SCNAs in clusters A and B patients during bladder cancer evolution (Online Methods).
367 Among cluster A patients, 25 of 26 SMGs and 21 of 34 arm-level SCNAs were acquired at
368 the early and intermediate/late evolution stages, respectively (**Fig. 4a**). Among cluster B
369 patients, 17 of 24 SMGs and 27 of 34 arm-level SCNAs were acquired at early and
370 intermediate/late evolution stages, respectively (**Fig. 4a**). These data further supported that
371 the clonal diversities of both clusters A and B patients were largely contributed by the large-
372 scale SCNAs acquired at late evolution stages. Several SCNAs, including del(9),
373 del(17p), del(8p) and del(11p), were early clonal events shared by patients in both clusters A

374 and B while arm-level SCNAs, including del(4q), del(15q), del(10q),del(11q) and del(12),
375 were acquired at the early and late stages in clusters A and B, respectively (**Fig. 4a**).

376

377 To explore whether there were any other differences in the overall genomic landscapes
378 between clusters A and B patients, we firstly compared their non-silent somatic mutation
379 burdens and found no significance difference. The extent of intra-tumor heterogeneities as
380 measured by MATH values and Shannon entropy of CCFs in cluster A patients was
381 significantly higher than that of cluster B patients ($P < 0.001$, **Fig. 4a and Supplementary**
382 **Fig. 11**). We next estimated the overall burden of SCNAs at the chromosome/arm/focal
383 levels for each patient and showed that cluster A patients had significant higher burden of
384 large-scale SCNAs (arm & chromosome levels) but not focal SCNAs ($P < 0.001$, **Fig. 4d**).
385 Whole-genome doubling (WGD) events were prevalent in cluster A and patients with Asian
386 origin were enriched in cluster B (both $P < 0.001$). To be more specific, although our cohorts
387 included only a small number of NMIBC patients from Cohort 2, cluster B were enriched
388 with Cohort 2 NMIBC patients (51.0% in cluster B vs. 22.9% in cluster A, $P < 0.005$) and
389 Cohort 1 MIBC patients who were less likely to develop metastatic disease (52.6% in cluster
390 B vs. 33.3% in cluster A, $P < 0.001$, **Fig. 4a**). Further analysis of the overall survival for
391 Cohort 1 MIBC patients showed that patients in cluster A had worse survival rate than those
392 in cluster B after adjusting for WGD, racial origins as well as other clinical and genomic
393 parameters (**Fig. 4c**). These observations suggested that it was feasible to distinguish the
394 heterogeneous MIBC patients into two subtypes with distinct clinical outcomes based on
395 their inherited genomic architectures.

396

397 To further study whether high intra-tumor heterogeneity and chromosomal instability of
398 cluster A patients had influence on the tumor microenvironment, we compared the relative

399 expression levels of the immune signature genes among two genomic prognostic clusters
400 using ssGSEA (**Fig. 4e**). In Cohort 1, the infiltrating levels of Th17 cells and CD8+ T cells
401 were observed to be significantly higher in cluster B patients ($P < 0.001$ and $FDR < 0.1$, **Fig.**
402 **4e**). Previous studies proved that Th17 cells as subsets of T helper lymphocytes can mediate
403 the antitumor immune responses through interacting with effector CD8+ T cells²⁴. Cluster A
404 patients had significantly higher levels of infiltrating Th2 cells and Macrophages (Both $P <$
405 0.001 and $FDR < 0.1$, **Fig. 4e**), which had been proved to facilitate tumor growth and
406 metastasis leading to the reduced survival in the cancer²⁵⁻²⁷. These observations on
407 differences in tumor microenvironment between clusters A and B were also validated
408 independently in the Chinese cohort (**Fig. 4e**).

409

410 **DISCUSSION**

411

412 Bladder cancer, a heterogeneous group of diseases with high morbidity and mortality all over
413 the world, still lacks effective treatments and prognostic indicators. Copious epidemiological
414 evidence demonstrates the existence of great racial disparities in the incidence and prognosis
415 of bladder cancer. However, there were few studies investigating the molecular features of
416 bladder cancer patients across different racial populations. Mutational signatures are
417 reflective of previous exposures to various exogenous and endogenous mutagenic processes
418 during the lifetime of cancer evolution. The observed enrichment of clonal mutations in
419 APOBEC-a signature in our study further confirmed the tumorigenic roles of this signature
420 during the early stages of bladder cancer development²⁸⁻³⁰.

421

422 Notably, we also observed that the activities of several mutational signatures varied
423 substantially among different racial populations. Racial differences in exposures to

424 exogenous factors related to life history may account for some of the observed racial
425 differences in mutational signatures. The ARISTOLOCHIC signature could only be detected
426 in some Asian patients, especially those from Cohort 2. Herbs or products containing
427 aristolochic acids are widely consumed in some areas in Asia and the ARISTOLOCHIC
428 signature had been detected in several human cancers, including bladder cancer, renal cell
429 carcinoma and liver cancer, in previous studies in Asian patients³¹⁻³³. Our observation that
430 the ARISTOLOCHIC signature showed significant enrichment of subclonal mutations
431 indicated that this life history related signature was less likely to play important roles during
432 the early development of bladder cancer. In terms of the newly identified MMR-like
433 signature which also significantly enriched with subclonal mutations, more evidence was
434 needed to further exclude the potential influence of study batch effects on the observation of
435 this signature in a single study cohort.

436

437 Interestingly, our study also suggested the possible roles of racial differences in the
438 prevalence of gene mutations in mediating the racial disparities in the activities of mutational
439 signatures. It had been shown that mutations in *ERCC2* were associated with the activities of
440 COSMIC signature 5 in bladder cancer previously¹⁷. We showed that mutations in *ERCC2*
441 and other SMGs or pathways were associated with the activities of mutational signatures in
442 bladder cancer. APOBEC-a signature showed the highest activities in White patients and we
443 provided preliminary evidence showing that the high APOBEC-a signature activity was
444 associated with the high prevalence of somatic mutations in *AHNAK* in patients from the
445 White population. Future studies are needed to characterize the biology function of the
446 associations between mutations in SMGs or pathways and mutational signature activities to
447 establish the potential of utilizing the mutated genes such as *AHNAK* as biomarkers for the
448 clinical management of bladder cancer patients.

449

450 Previous studies had shown that high APOBEC-a signature activity was indicative of good
451 prognosis^{4,7,8}. In our analysis, we showed that clustering of the patients based on their
452 mutational signatures could stratify the patients into different prognostic subgroups. Batch
453 effects may have some influence on interpreting the results of cluster analysis of mutational
454 signatures in patients from different study sources. However, prognostic analysis was
455 performed for patients from Cohort 1 only in our study, which means that all the results of
456 survival analysis were less likely to be affected by batch effects. Although survival
457 information was not available for the NMIBC patients from Cohort 2, it had been well known
458 that NMIBC patients usually can survive with the disease for quite a long time. We assumed
459 that the observed clustering of a subset of Cohort 1 MIBC patients who had better survival
460 with NMIBC patients from Cohort 2 in prognostic analysis cannot be explained by batch
461 effects solely.

462

463 Trans-ancestry analysis of the genomic features of bladder cancer revealed that all the SMGs
464 were enriched with clonal mutations but a large number of arm- or chromosome-level
465 SCNAs were subclonal events. Thus, clonal defects of the SMGs may play pivotal roles in
466 the early evolution stages of bladder cancer. Clonal mutations in SMGs (such as *TP53* and
467 *ATM*) regulating the DNA repair machinery further lead to the accumulation of an abundant
468 of SCNAs which provides the rich resources fostering the clonal diversity and inter-
469 population heterogeneity of bladder cancer. The prevalence of *TP53* and *ATM* clonal
470 mutations varied greatly among Whites/Blacks/Asians, which may contribute to the
471 diversified overall burden of SCNAs as well as the inter-population differences in the
472 prevalence of individual clonal/subclonal SCNA events. Interestingly, when we performed
473 trans-ancestry molecular subtyping based on the genomic architectures of patients from

474 different populations, we identified a trans-ancestry prognostic subtype that were enriched
475 with Asian NMIBC patients and White/Black/Asian MIBC patients who tend to harbor
476 defects in driver genes, such as *FGFR3*, *HRAS* and *NFE2L2*, showing significant racial
477 differences in mutation prevalence among low-staged patients. These findings demonstrated
478 the feasibility of identifying trans-ancestry prognostic or even therapeutic subtypes based on
479 their genomic architectures, despite of the fact that the genomic features of bladder cancer
480 varied greatly among different populations.

481

482 The long-term survival rates for the MIBC patients are generally much lower than the
483 NMIBC patients who usually suffer from disease recurrence but rarely die of bladder
484 cancer²³. To reduce the risk of developing metastatic disease, MIBC patients are routinely
485 treated with cystectomy of the bladder, which is much more radical and invasive than
486 transurethral resection of bladder tumor currently used for treating NMIBC. Thus, it is
487 imperative to identify molecular markers or subtypes to predict the prognosis of MIBC for
488 guiding the clinical choice of treatments to improve the life-quality of bladder cancer
489 patients. Our study cohorts were mainly composed of MIBC patients from two studies
490 cohorts with different racial backgrounds and a small number of NMIBC patients from a
491 single cohort were also used as the external control for stratifying the MIBC patients into
492 prognostic subtypes. Only a few clonal or sub-clonal somatic events, including SMGs and
493 arm-level SCNAs, were potentially associated with the prognosis of MIBC in our study.
494 Previous studies showed evidence suggesting that a subset of MIBC patients shared similar
495 molecular features with the NMIBC patients whose genetic landscapes were characterized by
496 high prevalence of mutations in the *FGFR3*-Ras pathway and low burden of SCNAs³⁴.
497 Molecular subtypes of MIBC exhibiting similarities to NMIBC at the mRNA expression
498 level had been reported previously but the genetic causes underlying the dynamic changes at

499 expression levels between subtypes are not clear⁴. We analyzed the genomic architectures of
500 MIBC and NMIBC patients and selected the clonal/sub-clonal states of 60 potential driver
501 events as features of the prognostic subtypes. We identified two prognostic clusters of MIBC,
502 with the shorter overall survival subtype showing higher burden of large-scale SCNAs and
503 WGD, higher prevalence of mutations in *TP53* and *RBI*, higher levels of intra-tumor
504 heterogeneity as well as suppressed tumor microenvironment and higher rate of developing
505 metastatic disease. These findings highlighted the possibility of directing the clinical
506 management of MIBC patients based on their genomic architectures.

507

508 **ONLINE METHODS**

509

510 **Data sources and sample information**

511 Raw whole-exome sequencing, RNA-seq data and clinical information on the Chinese
512 bladder cancer patients were downloaded from the Sequence Read Archive (SRA063495)⁷.
513 Whole exome sequencing bam files, gene expression read counts and clinical information in
514 the TCGA-BLCA cohort were downloaded from the Genomic Data Commons (GDC) data
515 portal (<http://gdc-portal.nci.nih.gov>). All bladder cancer patients were classified into the
516 NMIBC or MIBC subtype based on their TNM stages. Patients who had metastatic diseases
517 at the time of biopsy or within one year after biopsy were identified as metastatic and patients
518 who were followed up for at least one year and did not show metastatic diseases during the
519 entire follow up period were identified as non-metastatic. Data on WGD were downloaded
520 from the Genomic Data Commons (GDC) website ([https://gdc.cancer.gov/about-](https://gdc.cancer.gov/about-data/publications/panimmune)
521 [data/publications/panimmune](https://gdc.cancer.gov/about-data/publications/panimmune))³⁵. All bladder cancer patients were classified into Asian, black
522 and White populations based on their racial origins (**Supplementary Table 2 and 3**).

523

524 **Identification of SNVs and SCNAs**

525 Bam files for the tumor and matched normal samples were processed as input. Somatic
526 mutations were called by using Mutect2 software¹² and further filtered with a read depth of at
527 least 10x in the germline and tumor samples, a maximum of two variant supporting reads in
528 the germline, a minimum tumor variant allele frequency of 10% and a maximum germline
529 variant allele frequency of 2%. Allelic SCNAs were called with the ReCapSeg software
530 following the Broad's GATK documentation
531 (<http://gatkforums.broadinstitute.org/categories/recapseg-documentation>).

532

533 **Estimation of intratumor genetic heterogeneity**

534 To estimate the level of intratumor genetic heterogeneity in bladder cancer, we calculated
535 each tumor's MATH value from the median absolute deviation (MAD) and the median of its
536 mutant-allele fractions at somatically mutated loci: $MATH=100*MAD/median$ ³⁶.

537

538 **RNA-seq analysis and estimation of immune cell score**

539 Bam files for paired samples were processed to quantify the transcript abundance levels by
540 using kallisto³⁷. We then used tximport³⁸ R package to convert transcript level value into
541 gene level. We used signature genes from previous study³⁹ to infer the infiltration levels of
542 different types of immune cells using ssGSEA⁴⁰. Normalized RNA-seq datasets were
543 provided as the inputs for the execution with 'gsva (data, list of signatures, method
544 = "ssgsea")'⁴¹.

545

546 **Mutation significance analysis**

547 MutSig2CV algorithm^{42,43} was used to identify the SMGs which were further filtered with P
548 < 0.05 & $q < 0.1$. A SMG should express in above 75% of the TCGA-BLCA patients and

549 with at least three read counts. Also, they should be reported as the census of human cancer
550 genes (<https://cancer.sanger.ac.uk/census>, version: 4_08_47_12_2018).

551

552 **Mutation clonality analysis**

553 We used the updated version of ABSOLUTEv1.2 algorithm^{44,45} with allelic copy number and
554 mutation data as inputs to infer the ploidies and CCFs of tumor cells. SNVs and SCNAs were
555 defined as clonal if the probabilities of observing CCFs ≥ 0.95 were greater than 0.5
556 ($\Pr_{(\text{CCF} \geq 0.95)} > 0.5$) or sub-clonal otherwise^{46,47}. To assess whether a specific gene or arm
557 level event was enriched with clonal or sub-clonal mutations, we used permutation tests
558 repeated by 10000 times to obtain a p value of clonal enrichment by dividing the times when
559 the observed clonal/sub-clonal ratio was greater than the expected ratio by 10000. We applied
560 the method of constructing the potential temporal order of mutation acquisitions during tumor
561 evolution⁴⁸.

562

563 **Mutational signature analysis**

564 We applied a Bayesian variant of NMF (BayesNMF) with the functions of optimal inference
565 for the number of signatures and *de novo* signature discovery to identify the mutational
566 signatures¹⁷. Comparison of the signatures extracted from three populations (Asian, Black
567 and White) and 30 COSMIC signatures was performed using the standard hierarchical
568 clustering R package with a distance measurement of ‘cosine’ similarity or ‘pearson’
569 correlation. The MSig clustering analysis was performed using a standard hierarchical
570 clustering in R, with a ‘euclidian’ distance for the signature activity matrix and a ‘ward.D’
571 linkage tree. By using the Elbow method to look at the total within-cluster sum of square
572 (wss) as a function of the number of clusters, the number of MSig clusters ($K = 4$) was
573 chosen so that adding another cluster does not improve much better the total wss.

574

575 **Signature enrichment analysis**

576 To search for genes whose mutation statuses were associated with the activity of a specific
577 signature, we applied a permutation statistical test¹⁷ to compare, for each gene, the signature
578 activities between samples with and without mutations in the gene. Firstly, to remove the
579 inflation in the number of mutations in each gene associated with the elevated background
580 mutation rates, we randomly produced a total of 10^4 permuted mutation matrix in which the
581 total counts of gene-specific and sample-specific mutations were kept the same as those
582 observed in our patient cohorts, following an approach described by Strona *et al*⁴⁹. We used
583 the one-tailed Wilcoxon rank-sum P value to compare the signature activity between mutant
584 and wild type samples of a specific gene. To get the final P value for a given gene, we
585 calculated the fraction of permuted matrix with a test P value equal to or more extreme than
586 the observed matrix (Sum of $P_{\text{observed}} \geq P_{\text{random}}$ times/the total number of permutations). To
587 increase the computational efficiency, we analyzed only 174 genes with a non-silent mutation
588 frequency of 5% or above, 26 SMGs, the APOBEC family member gene sets and the human
589 DNA repair gene sets that had been reported to be associated with some mutational signature
590 activities (downloaded from [https://www.mdanderson.org/documents/Labs/Wood-](https://www.mdanderson.org/documents/Labs/Wood-Laboratory/human-dna-repair-genes.html)
591 [Laboratory/human-dna-repair-genes.html](https://www.mdanderson.org/documents/Labs/Wood-Laboratory/human-dna-repair-genes.html)). We corrected for multiple-hypothesis testing
592 using the Benjamini-Hochberg procedure and used FDR $q < 0.1$ as the significance threshold.

593

594 **Calculation of the SCNA scores**

595

596 We calculated the SCNA scores according to a previous study with minor modifications⁵⁰.
597 Our calculation of SCNA was based on the integer allelic copy number calls generated by
598 ABSOLUTE⁵¹ which took the tumor purities into consideration. The absolute copy number

599 of each segment was determined and a chromosomal arm event would be called out if the
600 cumulative length of the deletions (genomic segments with minor alleles of 0 copy) or
601 amplifications (genomic segments with major alleles of 2 or more copies) on this arm was
602 greater than 50% of the chromosome arm. Chromosome level events were distinguished from
603 arm level events when both arms of a chromosome had the same copy number changes (in
604 sign). After excluding the arm- and chromosome-level copy number changes, the remaining
605 segments with SCNAs were defined as focal changes. Based on the copy number change sign
606 associated with each segment x of a chromosome, arm and focal event t , the assigned score S
607 were defined as:

608

$$609 \quad S_x = \begin{cases} +2 & \text{one allele had amplification and the another one had deletion} \\ +1 & \text{both the major and minor alleles had amplifications or deletions} \\ & +1 \text{ one of major and minor allele was in normal state} \\ & 0 \text{ both major and minor alleles were in normal state} \end{cases}$$

610

611 The sum score of deletions or amplifications at the chromosome ($ChromL$), arm ($ArmL$), and
612 focal levels ($FocalL$), were calculated separately:

613

$$614 \quad ChromL = \sum_{t \in Chrom} S_x$$

615

$$616 \quad ArmL = \sum_{t \in Arm} S_x$$

617

$$618 \quad FocalL = \sum_{t \in Focal} S_x$$

619

620 The *ChromL*, *ArmL* and *FocalL* scores of each tumor sample were normalized to the mean
621 and standard deviation calculated among all samples. In addition, we divided the summed
622 score of all SCNA segments by the total length of genomic segments to get “total normalized
623 SCNA level” score for each tumor sample, which represented the integrated level of SCNAs
624 among the genome⁵².

625

626 **Unsupervised clustering based on genomic architecture**

627 We used the CCFs of 26 SMGs and frequent arm level SCNAs to create a numerical matrix
628 (samples as columns) and then applied the NMF ‘lee’ algorithm to perform molecular
629 subtyping of bladder cancer. After manual inspection we chose the $K = 2$ solution and
630 reported two clusters (clusters A vs B).

631

632 **Statistical analysis**

633 Two-sided Mann-Whitney and Fisher’s exact tests were performed with the R functions
634 `Wilcox.test` and `chisq.test` to generate the empirical P values, respectively. P values were
635 adjusted for multiple hypothesis tests using the R function `p.adjust` with the “fdr” option

636

637 **Survival analysis**

638 Asian bladder cancer patients from Asia cohort were excluded in survival analysis due to the
639 lack of some key clinical information. Chi-square test statistics in Kaplan-Meier curves were
640 computed using log-rank tests. P values were also calculated from multivariate Cox
641 proportional-hazards regression models using the R package “survival”.

642

643 **Data availability**

644 Any relevant data are available from the authors upon reasonable request. The raw
645 sequencing data used in this manuscript are all publicly available (SRA063495 and Genomic
646 Data Commons (GDC) data portal (<http://gdc-portal.nci.nih.gov>)). The data produced by the
647 analysis in this manuscript are summarised in the Supplementary Tables and Supplementary
648 Data.

649

650 **Code availability**

651 All custom code used in this work is available from the corresponding authors upon
652 reasonable request.

653

654 **Competing interests:** The authors declare no competing interests.

655

656 **Author contributions**

657 B.F.Z. and Y.H. conceived the study. B.F.Z. and X.C.L. performed the bioinformatics
658 analysis. G.S.P., P.L.J. and Z.M.Z. downloaded and processed TCGA-BLCA data. C.X.W.,
659 S.D. and S.N.P. performed GSEA analysis. B.F.Z. and Y.H. wrote the manuscript. B.F.Z.,
660 J.Y.W., X.Y. and Y.H. revised the manuscript.

661

662 **Funding:** This study was supported by Shenzhen municipal government
663 (JCYJ20160429093033251)

664

665

666

667

668

669 **REFERENCES**

670

- 671 1. Ferlay, J. *et al.* Cancer incidence and mortality worldwide: sources, methods and
672 major patterns in GLOBOCAN 2012. *Int. J. cancer* **136**, E359–E386 (2015).
- 673 2. Sylvester, R. J. *et al.* Predicting recurrence and progression in individual patients with
674 stage Ta T1 bladder cancer using EORTC risk tables: a combined analysis of 2596
675 patients from seven EORTC trials. *Eur. Urol.* **49**, 466–477 (2006).
- 676 3. Fernandez-Gomez, J. *et al.* Predicting nonmuscle invasive bladder cancer recurrence
677 and progression in patients treated with bacillus Calmette-Guerin: the CUETO scoring
678 model. *J. Urol.* **182**, 2195–2203 (2009).
- 679 4. Robertson, A. G. *et al.* Comprehensive molecular characterization of muscle-invasive
680 bladder cancer. *Cell* **171**, 540-556. e25 (2017).
- 681 5. Hedegaard, J. *et al.* Comprehensive Transcriptional Analysis of Early-Stage Urothelial
682 Carcinoma. *Cancer Cell* (2016) doi:10.1016/j.ccell.2016.05.004.
- 683 6. Weinstein, J. N. *et al.* Comprehensive molecular characterization of urothelial bladder
684 carcinoma. *Nature* **507**, 315–322 (2014).
- 685 7. Guo, G. *et al.* Whole-genome and whole-exome sequencing of bladder cancer
686 identifies frequent alterations in genes involved in sister chromatid cohesion and
687 segregation. *Nat. Genet.* **45**, 1459 (2013).
- 688 8. Gui, Y. *et al.* Frequent mutations of chromatin remodeling genes in transitional cell
689 carcinoma of the bladder. *Nat. Genet.* **43**, 875 (2011).
- 690 9. Faltas, B. M. *et al.* Clonal evolution of chemotherapy-resistant urothelial carcinoma.
691 *Nat. Genet.* **48**, 1490–1499 (2016).
- 692 10. Yee, D. S., Ishill, N. M., Lowrance, W. T., Herr, H. W. & Elkin, E. B. Ethnic
693 differences in bladder cancer survival. *Urology* **78**, 544–549 (2011).

- 694 11. Gandomani, H. S. *et al.* Essentials of bladder cancer worldwide: incidence, mortality
695 rate and risk factors. *Biomed. Res. Ther.* **4**, 1638 (2017).
- 696 12. Cibulskis, K. *et al.* Sensitive detection of somatic point mutations in impure and
697 heterogeneous cancer samples. *Nat. Biotechnol.* **31**, 213–219 (2013).
- 698 13. Lichtenstein, L., Woolf, B., MacBeth, A., Birsoy, O. & Lennon, N. ReCapSeg:
699 Validation of somatic copy number alterations for CLIA whole exome sequencing.
700 (2016).
- 701 14. Health, N. *et al.* Signatures of mutational processes in human cancer. *Nature* **500**, 1–
702 108 (2013).
- 703 15. Alexandrov, L. B. & Stratton, M. R. Mutational signatures: the patterns of somatic
704 mutations hidden in cancer genomes. *Curr. Opin. Genet. Dev.* **24**, 52–60 (2014).
- 705 16. Alexandrov, L. B., Nik-Zainal, S., Wedge, D. C., Campbell, P. J. & Stratton, M. R.
706 Deciphering signatures of mutational processes operative in human cancer. *Cell Rep.*
707 **3**, 246–259 (2013).
- 708 17. Kim, J. *et al.* Somatic ERCC2 mutations are associated with a distinct genomic
709 signature in urothelial tumors. *Nat. Genet.* (2016).
- 710 18. Lee, I. H. *et al.* Ahnak functions as a tumor suppressor via modulation of TGFβ/Smad
711 signaling pathway. *Oncogene* **33**, 4675 (2014).
- 712 19. Futreal, P. A. *et al.* A census of human cancer genes. *Nat. Rev. cancer* **4**, 177 (2004).
- 713 20. Robertson, A. G. *et al.* Comprehensive Molecular Characterization of Muscle-Invasive
714 Bladder Cancer. *Cell* **171**, 540-556.e25 (2017).
- 715 21. Gui, Y. *et al.* Frequent mutations of chromatin remodeling genes in transitional cell
716 carcinoma of the bladder. *Nat. Genet.* **43**, 875–878 (2011).
- 717 22. Guo, G. *et al.* Whole-genome and whole-exome sequencing of bladder cancer
718 identifies frequent alterations in genes involved in sister chromatid cohesion and

- 719 segregation. *Nat. Genet.* **45**, 1459–1463 (2013).
- 720 23. Soria, F., Moschini, M., Korn, S. & Shariat, S. F. How to optimally manage elderly
721 bladder cancer patients? *Translational Andrology and Urology* vol. 5 683–691 (2016).
- 722 24. Asadzadeh, Z. *et al.* The paradox of Th17 cell functions in tumor immunity. *Cell.*
723 *Immunol.* (2017).
- 724 25. De Monte, L. *et al.* Intratumor T helper type 2 cell infiltrate correlates with cancer-
725 associated fibroblast thymic stromal lymphopoietin production and reduced survival in
726 pancreatic cancer. *J. Exp. Med.* **208**, 469–478 (2011).
- 727 26. Ostuni, R., Kratochvill, F., Murray, P. J. & Natoli, G. Macrophages and cancer: from
728 mechanisms to therapeutic implications. *Trends Immunol.* **36**, 229–239 (2015).
- 729 27. Walker, J. A. & McKenzie, A. N. J. T H 2 cell development and function. *Nat. Rev.*
730 *Immunol.* **18**, 121 (2018).
- 731 28. McGranahan, N. *et al.* Clonal status of actionable driver events and the timing of
732 mutational processes in cancer evolution. *Sci. Transl. Med.* **7**, 283ra54–283ra54
733 (2015).
- 734 29. Hedegaard, J. *et al.* Comprehensive Transcriptional Analysis of Early-Stage Urothelial
735 Carcinoma. *Cancer Cell* **30**, 27–42 (2016).
- 736 30. Lamy, P. *et al.* Paired exome analysis reveals clonal evolution and potential
737 therapeutic targets in urothelial carcinoma. *Cancer Res.* **76**, 5894–5906 (2016).
- 738 31. Poon, S. L. *et al.* Mutation signatures implicate aristolochic acid in bladder cancer
739 development. *Genome Med.* **7**, 38 (2015).
- 740 32. Hoang, M. L. *et al.* Aristolochic acid in the etiology of renal cell carcinoma. *Cancer*
741 *Epidemiol. Biomarkers Prev.* **25**, 1600–1608 (2016).
- 742 33. Ng, A. W. T. *et al.* Aristolochic acids and their derivatives are widely implicated in
743 liver cancers in Taiwan and throughout Asia. *Sci. Transl. Med.* **9**, (2017).

- 744 34. Felsenstein, K. M. & Theodorescu, D. Precision medicine for urothelial bladder
745 cancer: Update on tumour genomics and immunotherapy. *Nat. Rev. Urol.* **15**, 92–111
746 (2018).
- 747 35. Thorsson, V. *et al.* The immune landscape of cancer. *Immunity* **48**, 812-830. e14
748 (2018).
- 749 36. Mroz, E. A. & Rocco, J. W. MATH, a novel measure of intratumor genetic
750 heterogeneity, is high in poor-outcome classes of head and neck squamous cell
751 carcinoma. *Oral Oncol.* **49**, 211–215 (2013).
- 752 37. Bray, N. L., Pimentel, H., Melsted, P. & Pachter, L. Near-optimal probabilistic RNA-
753 seq quantification. *Nat. Biotechnol.* **34**, 525 (2016).
- 754 38. Sonesson, C., Love, M. I. & Robinson, M. D. Differential analyses for RNA-seq:
755 transcript-level estimates improve gene-level inferences. *F1000Research* **4**, (2015).
- 756 39. Şenbabaoğlu, Y. *et al.* Tumor immune microenvironment characterization in clear cell
757 renal cell carcinoma identifies prognostic and immunotherapeutically relevant
758 messenger RNA signatures. *Genome Biol.* **17**, 231 (2016).
- 759 40. Barbie, D. A. *et al.* Systematic RNA interference reveals that oncogenic KRAS-driven
760 cancers require TBK1. *Nature* **462**, 108 (2009).
- 761 41. Hänzelmann, S., Castelo, R. & Guinney, J. GSEA: gene set variation analysis for
762 microarray and RNA-seq data. *BMC Bioinformatics* **14**, 7 (2013).
- 763 42. Lawrence, M. S. *et al.* Discovery and saturation analysis of cancer genes across 21
764 tumour types. *Nature* **505**, 495 (2014).
- 765 43. Lawrence, M. S. *et al.* Mutational heterogeneity in cancer and the search for new
766 cancer-associated genes. *Nature* **499**, 214 (2013).
- 767 44. Carter, S. L. *et al.* Absolute quantification of somatic DNA alterations in human
768 cancer. *Nat. Biotechnol.* **30**, 413–421 (2012).

- 769 45. Huang, Y. *et al.* Clonal architectures predict clinical outcome in clear cell renal cell
770 carcinoma. *Nat. Commun.* **10**, 1–10 (2019).
- 771 46. Lohr, J. G. *et al.* Widespread genetic heterogeneity in multiple myeloma: Implications
772 for targeted therapy. *Cancer Cell* **25**, 91–101 (2014).
- 773 47. Landau, D. A. *et al.* Evolution and impact of subclonal mutations in chronic
774 lymphocytic leukemia. *Cell* **152**, 714–726 (2013).
- 775 48. Wang, J. *et al.* Tumor evolutionary directed graphs and the history of chronic
776 lymphocytic leukemia. *Elife* **3**, e02869 (2014).
- 777 49. Strona, G., Nappo, D., Boccacci, F., Fattorini, S. & San-Miguel-Ayanz, J. A fast and
778 unbiased procedure to randomize ecological binary matrices with fixed row and
779 column totals. *Nat. Commun.* **5**, 4114 (2014).
- 780 50. Davoli, T., Uno, H., Wooten, E. C. & Elledge, S. J. Tumor aneuploidy correlates with
781 markers of immune evasion and with reduced response to immunotherapy. *Science*
782 (80-). **355**, eaaf8399 (2017).
- 783 51. Carter, S. L. *et al.* Absolute quantification of somatic DNA alterations in human
784 cancer. *Nat. Biotechnol.* **30**, 413–421 (2012).
- 785 52. Davoli, T., Uno, H., Wooten, E. C. & Elledge, S. J. Tumor aneuploidy correlates with
786 markers of immune evasion and with reduced response to immunotherapy. *Science*
787 (80-). **355**, eaaf8399 (2017).
- 788
- 789
- 790
- 791
- 792
- 793

794 Figure Legends

795

796 **Figure 1. Mutational signatures of bladder cancer among Asian-140, Black-23 and**
797 **White-324 populations.** (a) Unsupervised hierarchical clustering of signatures identified in
798 our cohorts and the 30 signatures described by COSMIC. (b) Differences in the mutational
799 signature activities among three populations. (c) Unsupervised hierarchical clustering of 487
800 samples (MSig clusters) based on the number of mutations assigned to the five mutational
801 processes. (d) Enriched signature features of the four MSig clusters. (e) Kaplan-Meier
802 survival analysis of the four MSig clusters. (f) Multivariate Cox regressions analysis of
803 survival by including MSig clusters, racial origins, age, gender and TNM stage.

804

805 **Figure 2. Gene mutations associated with signature activities.** (a) Mutation enrichment
806 analysis identifies an association between four somatically mutated genes and signature
807 activities. (b) Comparison of the estimated numbers of signature mutations in tumors with
808 wild-type versus mutant *AHNAK/ERCC2/HRAS*. (c) Different mutation frequencies of the
809 three genes among Asian/Black/White populations.

810

811 **Figure 3. Racial difference in SMG mutations and SCNAs.** (a) The prevalence of
812 mutations in SMGs across races. (b) SMGs showing significantly different mutation
813 frequencies in different populations. (c) The overall burden of SCNAs in different
814 populations. (d) The prevalence of SCNAs across race groups. (e) Chromosome- or arm-level
815 SCNAs showing great racial disparities.

816

817 **Figure 4. Prognostic subtypes of bladder cancer with distinct genomic architectures.** (a)
818 Landscape of genomic architectures in 505 bladder cancer samples. (b) Kaplan-Meier

819 survival analysis of the two clonal subtypes. (c) Multivariate Cox regressions analysis of
820 survival by including clonal subtype, racial origins, WGD, MSig cluster, age, gender and
821 TNM stage. (d) Differences in the genome-wide/chromosome/arm and focal levels of SCNAs
822 scores between two subtypes. (e) Immune features of the two subtypes.

Figures

Fig 1

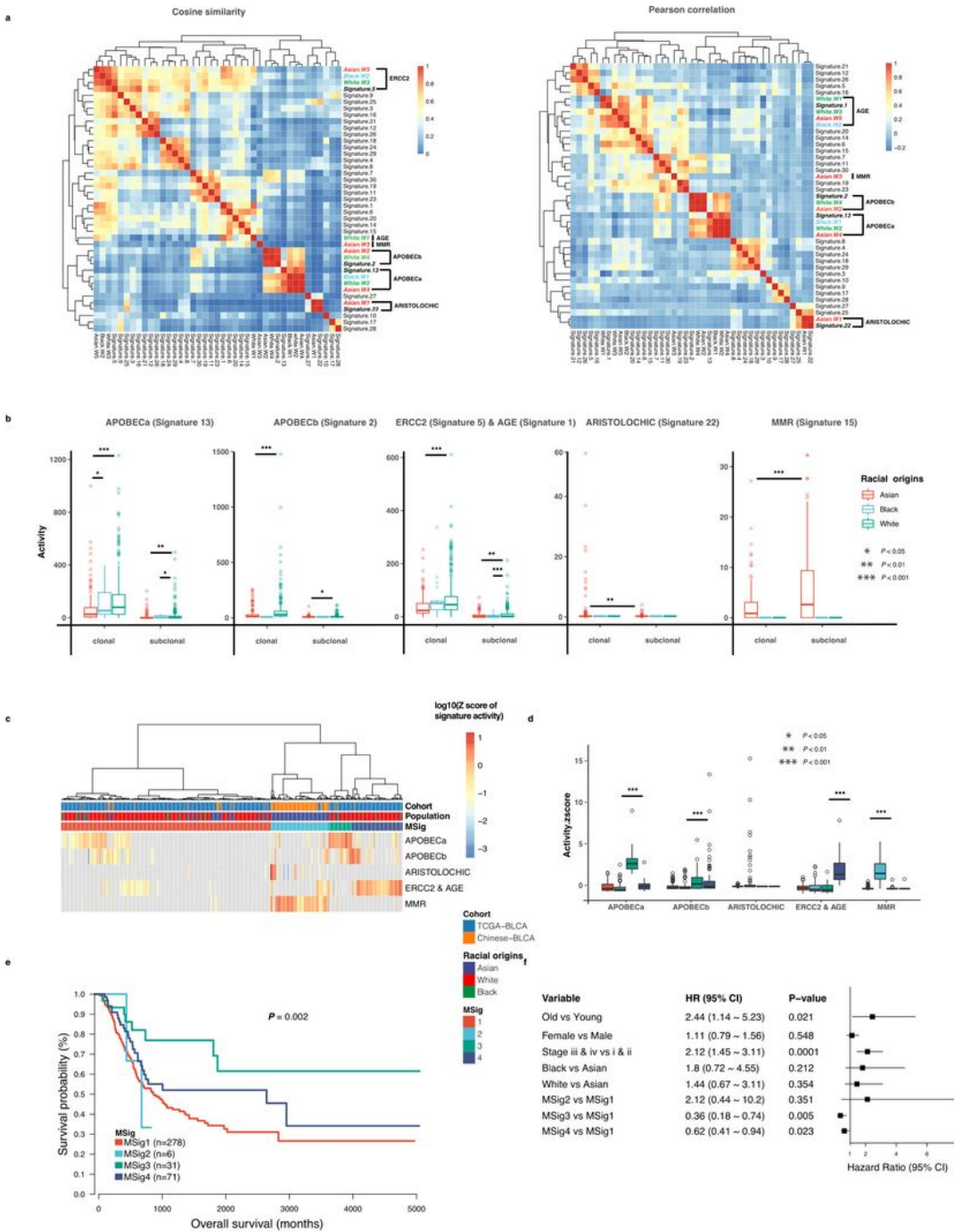


Figure 1

Mutational signatures of bladder cancer among Asian-140, Black-23 and White-324 populations. (a) Unsupervised hierarchical clustering of signatures identified in our cohorts and the 30 signatures described by COSMIC. (b) Differences in the mutational signature activities among three populations. (c)

Unsupervised hierarchical clustering of 487 samples (MSig clusters) based on the number of mutations assigned to the five mutational processes. (d) Enriched signature features of the four MSig clusters. (e) Kaplan-Meier survival analysis of the four MSig clusters. (f) Multivariate Cox regressions analysis of survival by including MSig clusters, racial origins, age, gender and TNM stage.

Fig 2

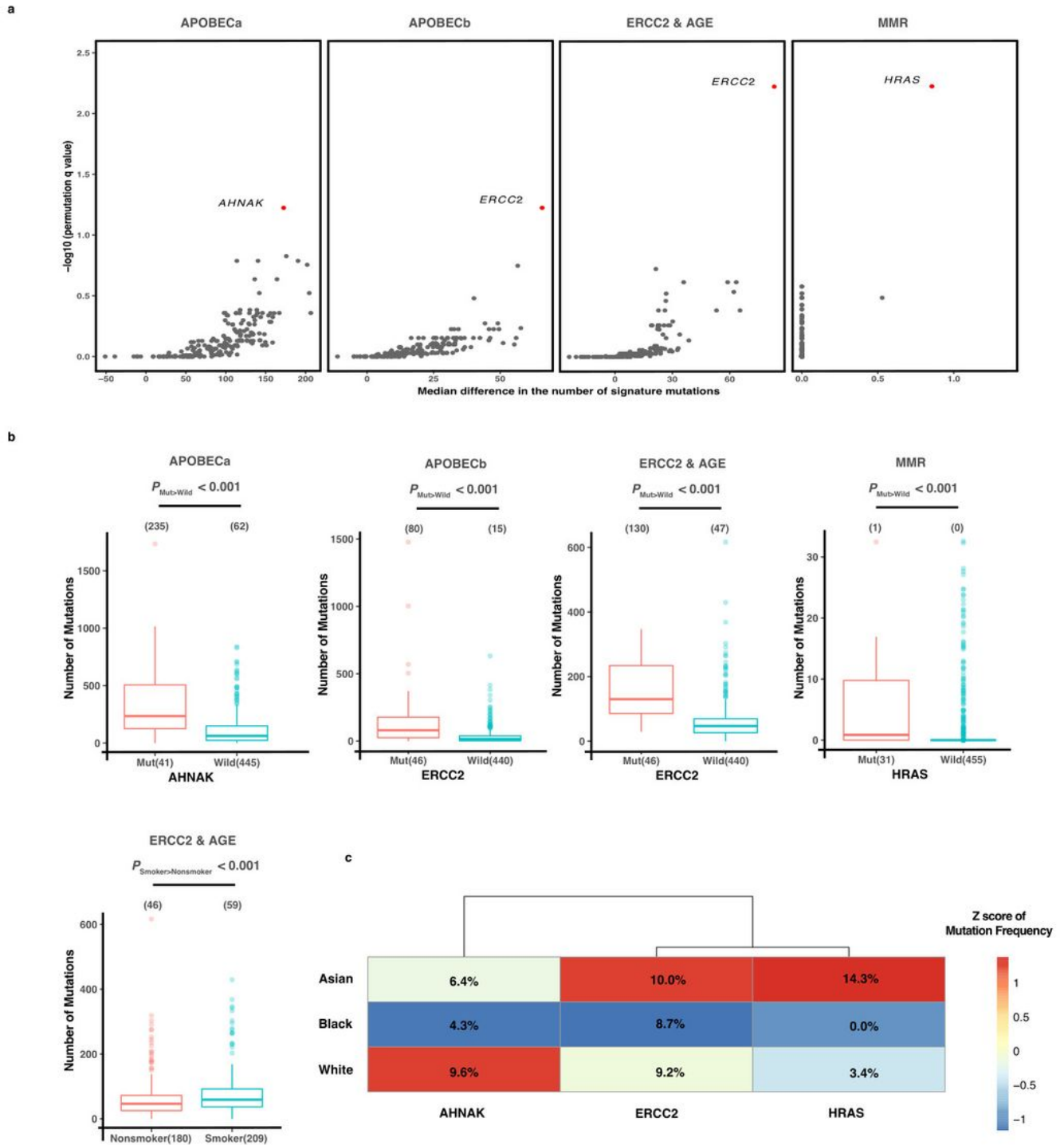


Figure 2

Gene mutations associated with signature activities. (a) Mutation enrichment analysis identifies an association between four somatically mutated genes and signature activities. (b) Comparison of the estimated numbers of signature mutations in tumors with wild-type versus mutant AHNK/ERCC2/HRAS. (c) Different mutation frequencies of the three genes among Asian/Black/White populations. (d) Different mutation frequencies of the three genes among Asian/Black/White populations.

Fig 3

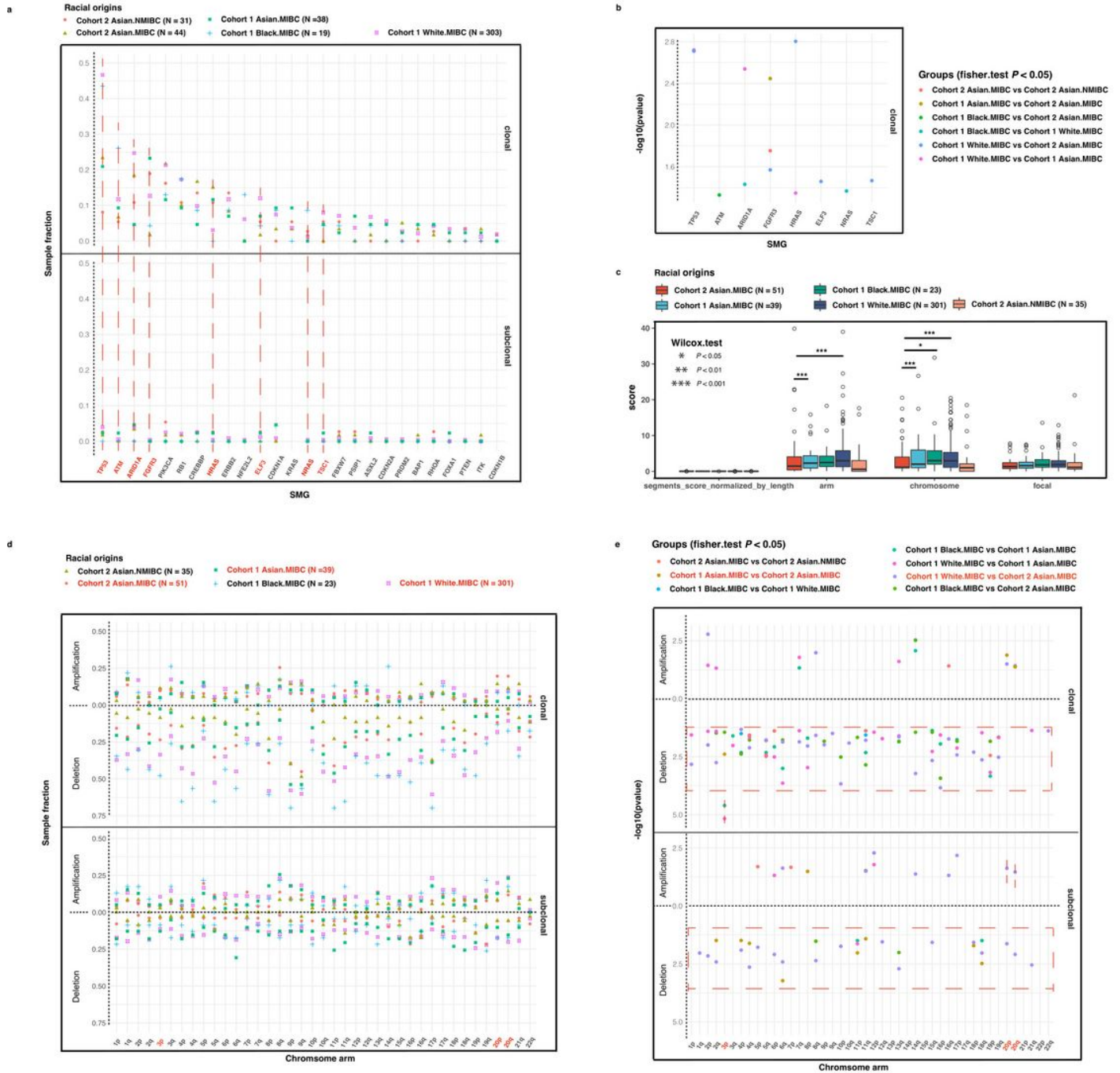


Figure 3

Racial difference in SMG mutations and SCNAs. (a) The prevalence of mutations in SMGs across races. (b) SMGs showing significantly different mutation frequencies in different populations. (c) The overall burden of SCNAs in different populations. (d) The prevalence of SCNAs across race groups. (e) Chromosome- or arm-level SCNAs showing great racial disparities.

Fig 4

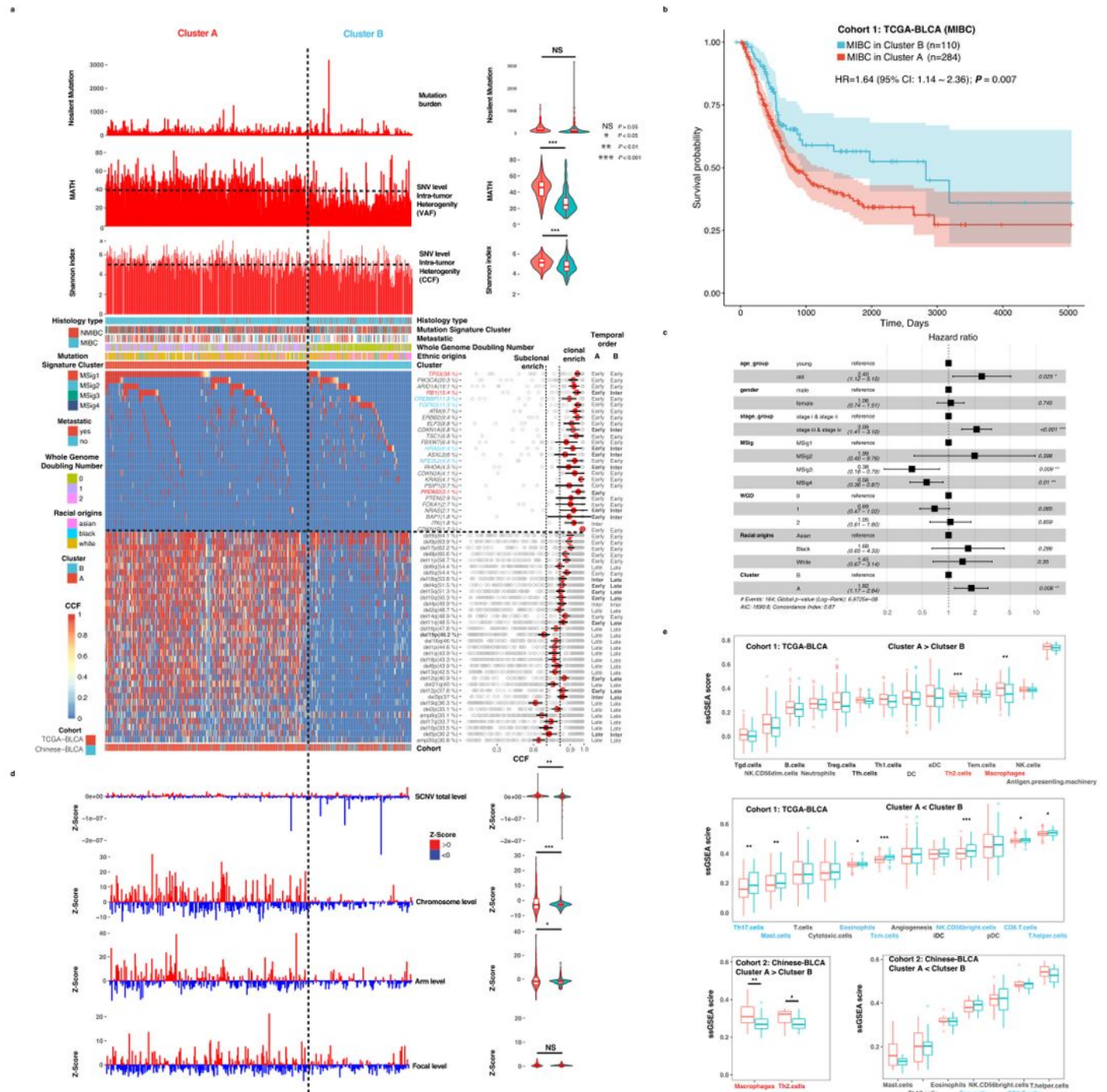


Figure 4

Prognostic subtypes of bladder cancer with distinct genomic architectures. (a) Landscape of genomic architectures in 505 bladder cancer samples. (b) Kaplan-Meier survival analysis of the two clonal subtypes. (c) Multivariate 819 Cox regressions analysis of survival by including clonal subtype, racial origins, WGD, MSig cluster, age, gender and TNM stage. (d) Differences in the genome-wide/chromosome/arm and focal levels of SCNAs scores between two subtypes. (e) Immune features of the two subtypes.

Supplementary Files

This is a list of supplementary files associated with this preprint. Click to download.

- [Table1.pdf](#)
- [SupplementaryData14.zip](#)
- [Supplementarymaterials.pdf](#)